Custom-Designed Fluxes for Refining Nickel Alloys

Yindong YANG, Mansoor BARATI and Alexander McLEAN
Department of Materials Science & Engineering
University of Toronto, Toronto, Ontario, Canada, M5S 3E4

Abstract: Nickel is a strategic metal widely used for the production of key materials. With the development of modern industry, the demand for nickel and nickel-alloys has dramatically increased and there is now a shortage of high-grade nickel resources. This poses a potential threat for the materials industry. Traditionally, nickel is produced by pyrometallurgical methods using nickel sulphide ore. However, good supplies of this mineral are decreasing and production of ferronickel from low-grade oxide ores as well as the recovery of nickel from spent catalysts generated are becoming widespread. Sulphur, phosphorus and arsenic are often found in these materials and the removal of such impurities during the production of nickel becomes an important issue. In this study, experiments were conducted with custom-designed fluxes that incorporated waste materials from the aluminum industry in order to remove sulphur, phosphorus and arsenic from nickel alloys without incurring a significant loss of other valuable elements. Effects of various factors, such as oxygen potential, temperature, slag composition, and additives, on the removal of the impurities were investigated. In this article, effectiveness of a single slag treatment for simultaneous removal of phosphorus, sulphur and arsenic from the nickel alloy is compared with a multi-slag treatment in which each impurity is removed under the most favourable conditions.

Key words: Arsenic, Phosphorus, Sulphur, Ferronickel, Nickel alloy, Nickel oxide, Red mud, Optical basicity, Usedcatalyst

1. Introduction

Nickel is one of the key elements used in stainless steel, heat-resisting alloys, catalysts, batteries, and nuclear industry. About 65% of Nickel consumption is for the production of stainless steel. Along with the increase of stainless steel production worldwide, the demand on nickel and nickel-alloys has dramatically increased. A shortage of nickel and its resources threatens the materials industry. Production of ferronickel from low-grade oxide ores and recovery of nickel from industrial waste products are two important strategies for increasing nickel supply. One of the major concerns in the production of ferronickel using nickel oxide ores through pyrometallurgical processes is the high sulphur level in the nickel alloy. Reportedly, the sulphur content in the ferronickel can be as high as 0.5%[1, 2]. Therefore, desulphurization of ferronickel becomes a key operation during ferronickel production from low-grade nickel oxide ores. In petroleum industry catalysts are used to remove arsenic and sulphur from crude oil and accelerate oil refining. The treatment of used catalysts will generate nickel alloys which contain high phosphorus, sulphur and arsenic. Removal of phosphorus, sulphur and arsenic are required. Fluxes with high refining capacity and low cost must be designed for the refining of ferronickel and nickel alloys for different applications.

Red mud is an iron-rich residue that is produced during the extraction of alumina from bauxite. About 2-4 tonnes of this material are generated for the production of one tonne of aluminum. Because of the size of this waste stream and its causticity, red mud is a major environmental concern. In most cases, the red mud is stored on location close to aluminum companies and a considerable amount of land is required for this purpose. Development of potential applications for this bauxite residue that would eliminate its impact on the environment and help restore contaminated sites is therefore an important consideration. The objective of the present study is to use waste materials from alumina production as the basis for an environment-friendly flux in the refining of ferronickel and nickel alloys in order to generate the nickel alloys with low residual levels of impurities. Fundamental of slag design for refining nickel alloy is discussed.

2. Fundamental consideration for ferronickel desulphurization and dephosphorization

2.1 Phosphate capacity of metallurgical slags

Searching for fluxes with high refining capacity and low cost is always of great interest in ferrous metallurgy. Based upon the dephosphorization reaction:

$$\frac{1}{2}P_2(g) + \frac{5}{4}O_2(g) + \frac{3}{2}(O^{2-}) = (PO_4^{3-}) \tag{1}$$

$$K_1 = \frac{a_{PO_4^{3-}}}{a_{O^{2-}}^{3/2} \cdot p_{P_2}^{1/2} \cdot p_{O_2}^{5/4}} \tag{2}$$

Wagner [3] defined the phosphate capacity of the slag as follows:

$$C_{PO_4^{3-}} = K_1 = \frac{(wt\%\ PO_4^{3-})}{p_{P_2}^{1/2} \cdot p_{O_2}^{5/4}} = \frac{K_1 a_{O^{2-}}^{3/2}}{f_{PO_4^{3-}}} \tag{3}$$

Taking into account the change of Gibb's free energy for dissolving phosphorus in liquid iron [4]:

$$\frac{1}{2}P_2(g) = [P]_{(1wt\%)} \quad \Delta G^\circ = -122352 - 19T \ \ (J) \tag{4}$$

A relationship between phosphate capacity and the phosphorus distribution ratio, L_P, can be derived and written as:

$$\log L_P = \log\frac{(wt\%\ P)}{[wt\%\ P]} = \log C_{PO_4^{3-}} + \log f_P + \frac{5}{4}\log p_{O_2} - \frac{6393}{T} - 1.476 \tag{5}$$

2.2 Sulphide capacity of metallurgical slags

Sulphide capacity is a useful parameter to compare the desulphurization ability of different slags. Once the sulphide capacity of the slag is known, a quantitative evaluation of desulphurization using the slag under a fixed condition can be made. It is also possible to design a slag with a favorable composition in order to achieve a desirable desulphurization result. The definition of sulphide capacity is commonly derived from the slag-gas exchange reaction:

$$\frac{1}{2}S_2(g) + O^{2-} = S^{2-} + \frac{1}{2}O_2(g) \quad (6)$$

$$K_6 = \frac{a_{S^{2-}} \cdot p_{O_2}^{1/2}}{a_{O^{2-}} \cdot p_{S_2}^{1/2}} \quad (7)$$

The sulphide capacity of the slag is defined as:

$$C_S = (wt\%\ S)\left(\frac{P_{O_2}}{P_{S_2}}\right)^{1/2} \quad (8)$$

Equation (8) can be rewritten in terms of the sulphur distribution ratio, L_S, by introducing the free energy change for the dissolution of gaseous sulphur into liquid iron:

Here f_S is sulphur activity coefficient in liquid iron. Dependence of final sulfur in metal, $[S]_f$, on initial sulphur in metal, $[S]_i$, L_S and slag to metal ratio, Q, is expressed as

$$\log L_S = \log\frac{(wt\%\ S)}{[wt\%\ S]} = \log C_{S^{2-}} + \log f_S - \frac{1}{2}\log p_{O_2} - \frac{7055}{T} + 1.224 \quad (9)$$

Equation (10) is derived based on mass balance between molten slag and liquid metal. A similar relationship holds for final phosphorus content of the metal.

$$[S]_f = \frac{[S]_i}{1 + L_S \cdot Q} \quad (10)$$

2.3 The concept and quantification of slag basicity

In discussing the refining capacities of slags, the ratio of basic oxides to acidic oxides expressed in weight percent, or sometimes as a molar ratio, is traditionally used as a measure of slag basicity. However the simple (CaO/SiO_2) ratio ignores the effects of other oxides and the ratio of ($CaO+MgO)/(SiO_2+Al_2O_3$) implies that lime and magnesia behave as equivalent basic oxides and that alumina and silica have the same degree of acidity. In order to show the importance of correct selection of slag basicity concept for slag property evaluation, an example is given as follow. Figure 1 shows the correlation of sulphide capacity of $CaO-MgO-SiO_2$ slags with the ratio of $B_2 = CaO/SiO_2$. Data used in this figure were derived from the work of Nzotta, Du Sichen and Seetharaman [5, 6]. As shown in this figure, the sulphide capacity of the slags increases with increasing CaO/SiO_2 ratio as expected. Figure 1 also shows that the slags with 20-30% MgO content have a higher sulphide capacity than other slags with the same CaO/SiO_2 ratio. However, when $B3=(CaO+MgO)/SiO_2$ is used to measure slag basicity, the opposite tendency is observed that the slags with 5% MgO have a higher sulphide capacity, as shown in Figure 2.

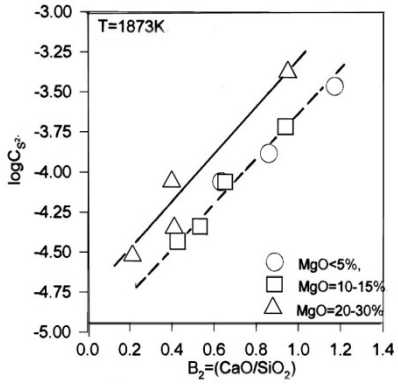

Figure 1, Dependence of sulphide capacity on CaO/SiO_2 ratio of CaO-MgO-SiO_2 slag at 1873K.

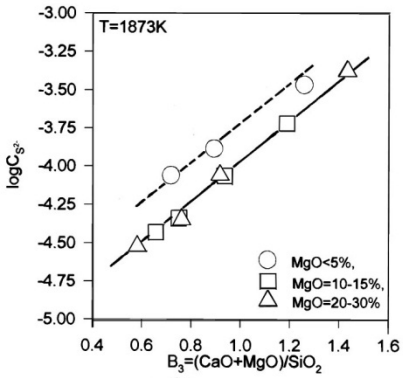

Figure 2, Dependence of sulphide capacity on $(CaO+MgO)/SiO_2$ ratio of CaO-MgO-SiO_2 slag at 1873K.

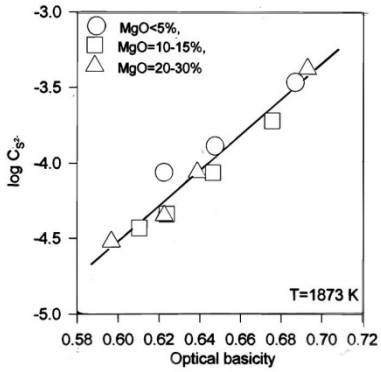

Figure 3, Dependence of sulphide capacity on optical basicity of CaO-MgO-SiO_2 slag at 1873K.

Optical basicity provides a good foundation for a better understanding of the behaviour of molten slags than the conventional basicity ratios. The concept of optical basicity was developed by glass scientistsand introduced to the metallurgical community by Duffy, Ingram and Sommerville in the late seventies [7, 8]. This approach has proved to be a valuable tool for designing slags or fluxes which will have the required characteristics with respect to the behaviour of, for example, sulphur, phosphorus, hydrogen, magnesia and alkalies[9-10]. Optical basicity of molten slag can be calculated using the following relationships:

$$\Lambda = \sum_{i=1}^{n} \Lambda_i N_i \tag{11}$$

Here Λ : Optical basicity of the slag

Λ_i : Optical basicity value of component "i"

N_i : Compositional fraction

$$N_i = \frac{X_i n_{oi}}{\sum_{i=1}^{n} X_i n_{oi}} \tag{12}$$

X_i : Mole fraction of component "i" in the slag

n_{Oi} : Number of oxygen atoms in component "i"

Figure 3 shows the relationship between sulphide capacity and optical basicity of slags using the same data shown in Figures 1 and 2. A good linear relationship is found between the two parameters for slags with different MgO contents. At 1873K, this relationship is given by:

$$log C_{S^{2-}} = 11.80\,\Lambda - 11.60 \qquad (R^2 = 0.94) \tag{13}$$

Comparing Figures 1, 2 and 3, it is again evident that optical basicity provides a good foundation for a better understanding of the behavior of molten slags than the conventional basicity ratios.

2.4 Custom-designed slags for hot metal and steel refining

Based on a great number of experimental data, an empirical relationship between phosphate capacity and optical basicity was obtained [11].

$$log C_{PO_4^{3-}} = \left(-\frac{36412}{T} + 37\right)\Lambda + \frac{71493}{T} - 30.8 \quad (14)$$

The above relationship can be used to design a slag with desired dephosphorization capacity in a temperature range from 1473 to 1773K and does not seem to be restricted to certain components.

For many years attempts have been made to correlate empirically the sulphide capacities of slags with different indices. From quantitative evaluations of desulphurization data for a number of different slag systems, empirical equation between sulphide capacity and optical basicity was obtained [10].

$$log C_{S^{2-}} = \left(\frac{22690 - 54640\Lambda}{T}\right) + 43.6\Lambda - 25.2 \quad (15)$$

Thus with the aid of the optical basicity model, an optimum slag composition can be designed for different operations in steelmaking in order to establish appropriate conditions to control the behaviour of phosphorus, sulphur as well as many other impurities. Using the fundamental information discussed in this section, slag can be designed for a significant desulphurization or dephosphorization or simultaneous desulphurization and dephosphorization. As an example, the flowsheet of slag design for hot metal and ferronickel desulphurization is described as follows: (1) Determine the L_S value when initial sulphur content and target final sulphur content are defined, and the ratio of slag to metal is fixed. (2) Calculate sulphide capacity of the designed slag when metal composition, oxygen partial pressure and refining temperature are fixed. (3) Calculate optical basicity of the slag designed using Equation (15) at the fixed temperature, (4) Calculate the slag compositions using the optical basicity of designed slag and optical basicity value of each component of the slag, (5) Checkslag melting behavior using phase diag or published information. The same procedure can be used to design a slag with optimum composition for hot metal dephosphorization.

3. Hot metal treatment using CaO-based fluxes

During the actual tests, hot metal or ferronickel was prepared by melting steel scrap (AISI 1117), nickel scrap, FeS and FeP in MgO crucibles or graphite crucibles depending on the carbon content required in the master alloy. The nickel hot metal after melting contained 2-5% carbon, 0-30% nickel, 0.03-0.05% P and 0.03-0.11% sulphur. The content of manganese and silicon was lower than 0.15% respectively. Four types of red mud from two different sources were used in this study and the chemical compositions are given in Table 1.

Table 1：Chemical compositions of red mud from different sources

No.	CaO	MgO	Na_2O	K_2O	Fe_2O_3	TiO_2	Al_2O_3	SiO_2	S	P_2O_5	Opt.B
Bay. 1	11.6	0.20	8.4	0.08	39.2	6.73	19.9	14.0	n.a	n.a	0.73
Bay. 2	3.4	0.28	10.5	0.05	40.9	6.79	21.4	16.9	n.a	n.a	0.73
Sint. 1	42.6	1.61	8.6	1.15	14.3	4.09	6.9	20.3	0.64	0.24	0.78
Sint. 2	43.0	1.10	3.6	0.58	19.2	4.49	7.48	19.3	0.39	0.26	0.73

Bay.1and Bay.2 are red mud from Bayer process obtained from different plants in Canada. Sint.1 and Sint.2 are red mud samples from the lime-sintering process, currently used in China. As shown in the table, red mud generated from Bayer process contains high iron oxide content, which is suitable for applications under oxidizing conditions, for example, dephosphorization of hot metal containing high phosphorus content (0.2-0.7% P) in Sweden. Red mud generated in lime sintering process contains a high CaO content and low iron oxide. The optical basicity of the by-product from lime sintering alumina production is from 0.73 to 0.78 depending on Na_2O content in the red mud, which is suitable for hot metal desulphurization under reducing conditions.

3.1 Hot metal desulphurization using red mud based flux under reducing condition

Preliminary experiments were carried out in a 10 KW induction furnace. In most of these experiments, 56g flux was added to 500 g hot metal. The flux contained 71% red mud from lime sintering process, 20% CaO and 9% reducing reagents. In order to limit the negative effect of iron oxide in the red mud on desulphurization, reduction reagents, such as aluminum or carbon powder, were used to control oxygen potential in the reaction system. Results are given in Figure 4. As shown in the figure, addition of aluminum is more powerful than carbon addition to improve desulphurization performance of the slags. Increasing temperature from 1673K to 1773K, desulphurization rate and degree increase significantly. When aluminum was added to the red mud based flux, hot metal temperature was increased by 15-20K due to the exothermic reaction between Fe_2O_3 and aluminum. Temperature drop and iron loss are two important concerns in hot metal pre-treatment process. Reduction of iron oxide in the red mud by aluminum can increase iron yield and reduce temperature drop, hence bring economic benefits for steelmaking process.

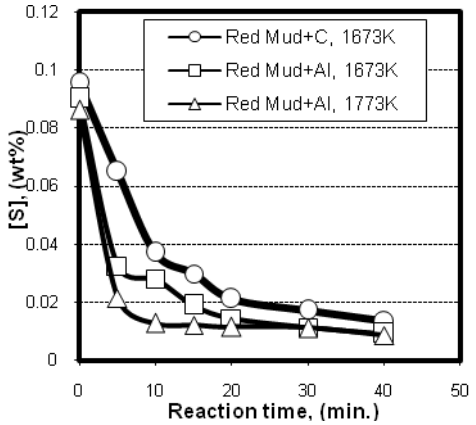

Figure 4, Hot metal desulphurization using red mud based fluxes under reducing conditions at different temperatures.

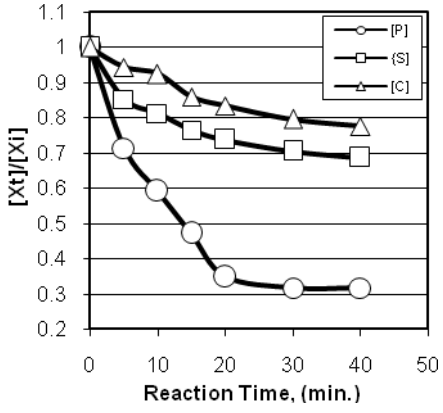

Figure 5, Hot metal simultaneous dephosphorization and desulphurization under controlled oxidizing conditions at 1623K.

3.2 Simultaneous desulphurization and dephosphorization under controlled oxygen potentials

These experiments were also carried out in a 10 KW induction furnace. Magnesia or Alumina crucibles were used as the container for liquid metal and molten slag. The flux containing 40 g red mud from sintering process, 10 g CaO and 20 g iron oxide was added to 250 g hot metal. Figure 5 shows the result of hot metal simultaneous desulphurization and dephosphorization under controlled oxidizing atmosphere. As shown in the figure, phosphorus in hot metal is reduced from 0.063% to 0.020%, sulphur is reduced from 0.074% to 0.05%, Dephosphorization and desulphurization degree reached 68% and 32% respectively. A small amount of carbon loss is found during hot metal treatment under oxidizing conditions. Carbon loss increases with increasing oxygen potential in the reaction system; therefore, it can be used as an indirect indicator of oxygen potential of the slags. The correlation of desulphurization and dephosphorization degree with the degree of carbon loss is shown in Figure 6. As shown in the figure, a simultaneous dephosphorization and desulphurization can be achieved when carbon loss is in the range from 10% to 20%. Effect of iron oxide addition to red mud based fluxes on desulphurisztion and dephosphorization are shown in Figure 7. As shown in the figure, in order to achieve a good dephosphorization, FeO content in the synthetic slag must be higher than 38%; When FeO in the slag is in the range from 30% to 40%, a good simultaneous dephosphorization and desulphurization can be achieved. Red mud from Bayer process contains about 40% FeO and 10% to 15% Na_2O, which can be used as a base for making synthetic slag for hot metal dephosphorization; while red mud from lime-sintering process can be used for hot metal desulphurization or simultaneous desulphurization and dephosphorization.

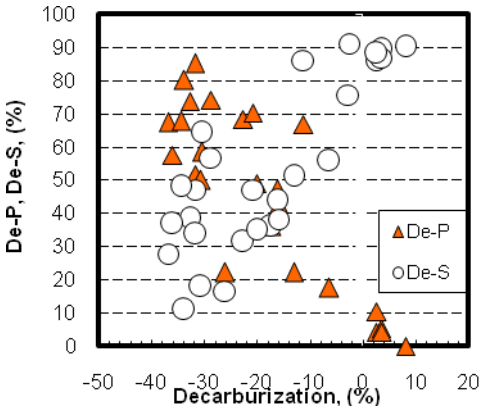

Figure 6, Relation between carbon loss and desulphurization and dephosphorization degrees.

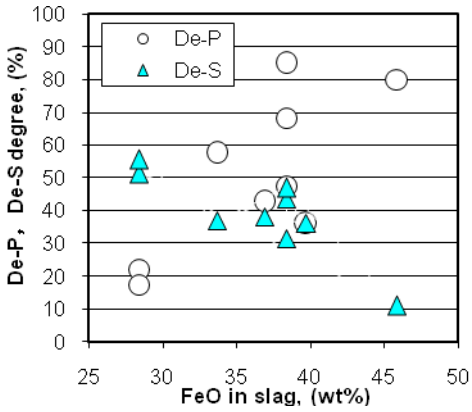

Figure 7, Effect of FeO content in slag on desulphurization and dephosphorization

Effect of oxygen partial pressure in the reaction system on phosphorus and sulphur distribution ratios can be calculated using Equations (5) and (9) at the fixed experimental conditions. During the calculation, hot metal with [C]=4%, [Si]<0.15%, [Mn]<0.15%, [P]=0.04-0.10%, [S]=0.04-0.10% and T=1623K were assumed. Activity coefficient of phosphorus, f_P, and sulphur, f_S, in the hot metal can be calculated using hot metal composition. Three slags with optical basicity of 0.75, 0.80 and 0.85 are selected for the calculation. Optical basicity of CaO-CaF_2 slag with CaO saturation is

about 0.75, which was traditionally used in steelmaking process. Optical basicity of red mud from lime-sintering process can reach 0.80 and 0.85 respectively depending on Na_2O and CaO contents in the slags. Sulphide and phosphate capacities of the three slags calculated using Equations (14) and (15) are given in Table 2.

Table 2：Calculated phosphate and sulphide capacities of various slags at 1623K

Fluxes	Optical B	Log Cp	Log Cs
$CaO\text{-}CaF_2$ based flux	0.75	24.4	-3.77
Red mud with 10% Na_2O,	0.80	25.1	-3.27
Red mud with 20% Na_2O	0.85	25.6	-2.78

Substituting the values of slag phosphate capacity, phosphorus activity coefficient in liquid metal, f_P and temperature in Equation (5), a relationship between phosphorus distribution ratio, $L_{p,}$ and oxygen partial pressure, $p_{O2,}$ for a fixed slag composition, that is for the fixed slag optical basicity, is obtained, as shown in Figure 8. In the same procedure, the dependence of L_s on p_{O2}, for a slag with a fixed composition can be calculated and the relationship is shown in the same figure. As seen, phosphorus distribution ratio increases and sulphur distribution ratio decreases with increasing oxygen partial pressure as expected, and they increase with increasing slag optical basicity. A simultaneous dephosphorization and desulphurization can be achieved at log p_{O2}= -15. The calculated result shown in Figure 8 is in good agreement with the tendency shown in Figures 6 and 7.

3.3 Effect of nickel on desulphurization

During these experiments, the nickel content in the hot metal was progressively increased from zero to 30%, which covers the range of nickel contents in the nickel pig iron (Ni=1-15%) produced by the blast furnace route using low-grade nickel oxide ore. As shown in Figure 9, with increasing nickel content in the hot metal, the degree of desulphurization is slightly reduced. After investigation it was found that with increasing nickel content in hot metal from 0 to 30%, carbon solubility in the nickel hot metal decreased from 4.8% to 3.8% at 1673K, see Figure 10.

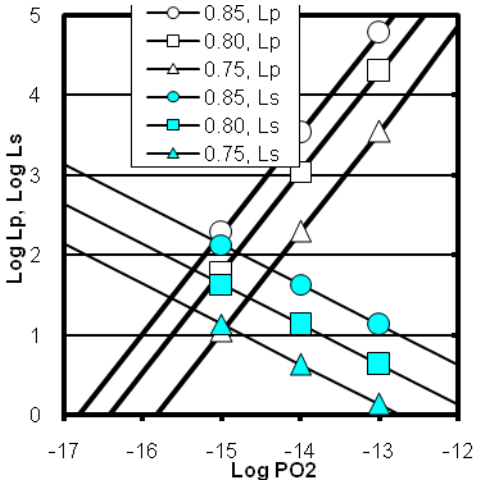

Figure 8, Dependence of L_P and L_S on oxygen partial pressures and slag optical bacicity at 1623K.

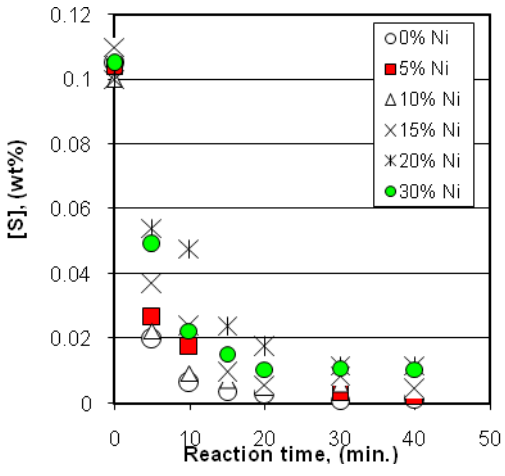

Figure 9, Effect of nickel content in hot metal on desulphurization at 1673K.

In order to confirm this observation, equilibrium experiments were carried out. A graphite crucible with five cells was used as a container for the liquid metal. Nickel and iron powders with purity higher than 99.9% were used to make hot metal with 0 to 30% nickel. In view of the strong stirring in the induction furnace, the holding time of the crucible at 1673K was 2 hours. At the end of the experiment, the graphite crucible with its contents was quickly withdrawn and quenched in water. The change in carbon concentration with nickel content after these equilibration experiments is included inFigure 10.

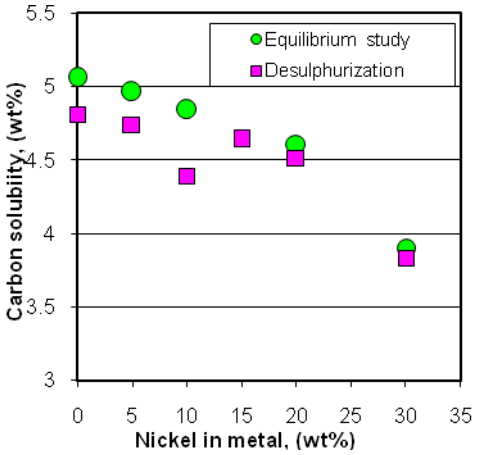

Figure 10, Effect of nickel in hot metal on carbon solubility at 1673K.

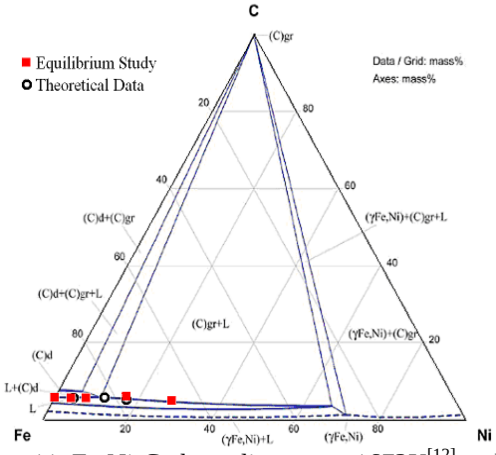

Figure 11, Fe-Ni-C phase diagram at 1673K[12] and the experimental data obtained in the present work.

As shown in Figure 10, the square symbols represent the carbon content in metal samples obtained during the desulphurization experiments, while the data shown by solid circles correspond to the carbon solubility values derived from the equilibrium experiments. Both sets of data provide confirmation that carbon solubility in hot metal decreases with increasing nickel content. As shown in the Fe-Ni-C ternary diagram, Figure 11, values for carbon solubility in Fe-Ni alloys obtained from the equilibrium study are in good agreement with data in the literature [12]. Since carbon in hot metal increases the sulphur activity, hot metal with high nickel content and therefore lower carbon content will generate melts with a lower sulphur activity, which as a consequence, would be expected to display a lower rate as well as a smaller amount of desulphurization.

3.4 Effect of aluminum addition

In order to limit the negative effect of iron oxide in the red mud on desulphurization and reduce oxygen potential in the reaction system, reduction reagents, such as aluminum and carbon powder, can be added to red mud based fluxes. Since aluminum is a relatively expensive additive compared to carbon, an optimum amount of aluminum addition is of interest. Experiments were carried out in the induction furnace. Flux containing 45.5g red mud from sintering process, 4.5g lime and different amounts of aluminum was added to 500g hot metal. Experimental conditions and procedure were the same as described before. The results obtained are shown in Figures 12 and 13.

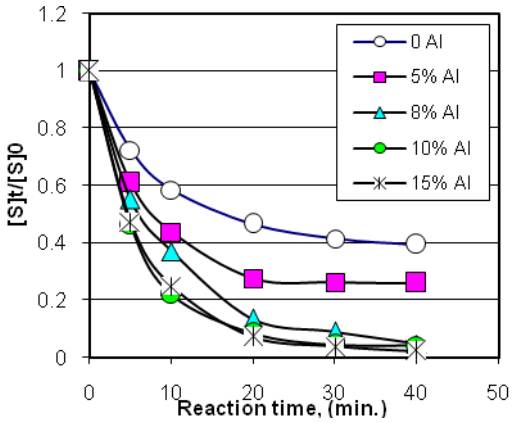

Figure 12, Effect of aluminum addition to red mud based flux on sulphur removal at 1673K.

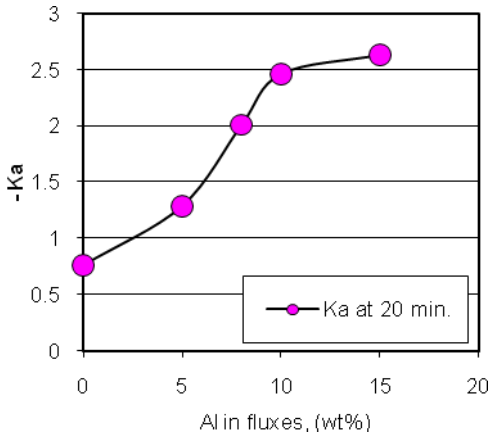

Figure 13, Effect of alumiium addition on desulphurization rate constant at 1673K.

As shown in Figures 12 and 13, with increasing aluminum addition from 0 to 10%, desulphurization rate shows a significant increase. However, a future increase of aluminum addition from 10% to 15% does not markedly improve desulphurization. Obviously, the amount of aluminum addition depends on iron oxide content in the red mud, and should be determined according to each situation.

4. Simultaneous removal of phosphorus, sulphur and arsenic from nickel alloy using CaC_2-CaF_2 slag

The chemical composition of the Ni-based alloy obtained from the treatment of used catalyst generated by the petroleum industry is given as: Ni=50.2%,Co=9.62%,V=9.05%, Fe=9.03%,Mo=6.36%, Si=2.54%, Cu=0.43%, C=0.42%, P=9.1%, S=0.39% and As=0.6%. Removal of impurities, such as P, S and As, could increase the value of the nickel alloy so that it could be used for other applications in metallurgy or re-used in the production of catalyst for petroleum industry.

Regarding the treatment of Ni-based alloy in this study, two treatmentroutes can be selected. One isthe traditional route that is a two or three slag practice, i.e. the phosphorus in Ni-basedalloy can be removed using conventional slag under oxidizing condition, then sulphur is removed under reducing condition using lime-based fluxes including red mud flux, and finally arsenic is removed with additions of CaSi or CaC_2under strong reducing condition. The other route is a one step operation to remove all impurities, S, As and P, by injection of the fluxes containing calcium under strong reducing condition. Considering the oxidizing loss of valuable elements, such as Ni, Co, V and Mo, from nickel alloy, the treatment of nickel alloy under oxidizing condition is not ideal form economic point of view. Therefore, a two or three slag practice is not recommended, and a one step operation under strong reducing condition to remove all three impurities, P, S and As, is favourable. When using the flux containing calcium for dephosphorization under strong reducing condition, dephosphorization reaction can be expressed as [13]:

$$3Ca(l) + P_2(g) = Ca_3P_2(s) \quad \Delta G^\circ = -653460 + 144.01\,T \quad (J/mol) \tag{16}$$

$$3CaO(s) + P_2(g) = Ca_3P_2(s) + \frac{3}{2}O_2(g) \quad \Delta G^\circ = -2046540 - 681T \quad (J/mol) \tag{17}$$

In order to achieve a good dephosphorization under reducing condition, the experiment must be carried out at a very low oxygen partial pressure and high temperature. A slag with high CaO activity or high calcium content should be selected. Addition of CaSi or CaC_2 to the CaO-based slag can continuously supply calcium to the slag.

The removal of phosphorus, sulphur and arsenic from iron-based alloy was studied by Min [14], Dong [15] and Liu [16]. A study on nickel alloy has not been reported. Min and Sano measured the standard Gibbs free energy of formation of Ca_3As_2 and the result obtained is given as [14].

$$3Ca(l) + 2As(l) = Ca_3As_2(s) \quad \Delta G^\circ = -723800 + 172.8\,T \quad (J/mol) \tag{18}$$

Experiments were carried out under reducing conditionsat 1673K using the fluxes with different ratios of CaC_2 to CaF_2. The amount of CaC_2-CaF_2 slag used in each experiment was 55g with the change of CaF_2content in the slag from 20% to 40%. The weight of nickel alloy melted was 150g. Graphite crucibles were used as containers for liquid alloy. Changes of $[I]_t/[I]_0$ ratio for some key elements in the liquid alloy with reaction time are shown in Figure 14. Here $[I]_t$ and $[I]_0$ represent "I' component (I=P, S and As) in the nickel alloy at any time of refining and at time zero respectively. By introducing this ratio, the changes of P, S and As can be shown on the same diagram even though the initial content of each element is different.

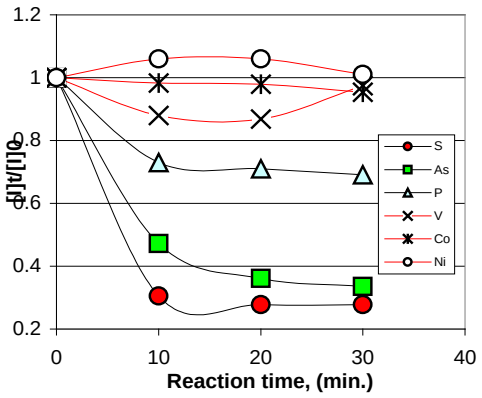

Figure 14, Changes of $[I]_t/[I]_0$ of some key elements in alloy with reaction time when using the flux with 70%CaC_2 and 30%CaF_2 at 1673K.

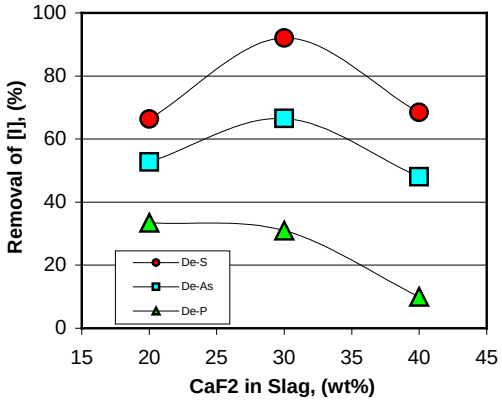

Figure 15, Effect of CaF_2 content in CaC_2-CaF_2 fluxes on removal ratio of some key elements in alloy during refining at 1673K.

As shown in Figure 14, simultaneous removal of phosphorus, sulphur and arsenic are achieved when using CaC_2-CaF_2 flux under strong reducing conditions. The valuable elements, such as nickel, vanadium and cobalt, have no change. Figure

15 shows the effect of CaF_2 addition to CaC_2 –CaF_2 flux on the removal of sulphur, arsenic and phosphorus. At 1673K a better refining result can be achieved when CaF_2 amount is 30% of the total flux. The role of CaF_2 in the CaC_2-CaF_2 slag is as a fluxing material. The flux with high CaC_2 content should have a high refining capacity, but the melting point of the flux is high, which will result in a poor kinetic condition for slag-metal reaction. As shown in Figure 15, more than 90% sulphur, 68% arsenic and 30% phosphorus could be removed through this single slag practice. Since the content of phosphorus in the nickel alloy is very high (9.1%), an absolute amount of phosphorus removal of 2.7% in weight percentage is significant.

5. Conclusions

With the aid of models based on theoretical analysis and experimental results, a method for custom-design of slag with optimum composition was introduced in order to maintain appropriate conditions to control the behaviour of phosphorus, sulphur as well as many other impurities. The fundamental information obtained in this study was tested in hot metal and ferronickel desulphurization and dephosphorization. A slag containing CaC_2 and CaF_2 was also designed for simultaneous removal of phosphorus, sulphur and arsenic from nickel alloys under strong reducing conditions.

References

[1] T. Watanabe, S. Ono, H. Arai and T. Matsumori, “Direct Reduction of Garnierite Ore for Production of Ferronickel with a Rotary Kiln at Nippon Yakin Kogyo Co., Ltd., Oheyama Works”, International Journal of Mineral Processing, 1987, Vol.19, pp.173-187.

[2] I.J. Kotze, “Pilot Plant Production of Ferronickel from Oxide Ores and Dust in a DC Arc Furnace”, Mineral Engineering, 2002, Vol.15, pp.1017-1022.

[3] C. Wagner, “The Concept of the Basicity of Slags”, Met. Trans., 1975, Vol. 6B, pp.405-409.

[4] E. T. Turkdogan: Physical Chemistry of High Temperature Technology, Academic Press, New York, 1980.

[5] M.M. Nzotta, R. Nilsson, Du Sichen and S. Seetharaman, Sulphide Capacities in MgO-SiO_2 and CaO-MgO-SiO_2 Slags, Ironmaking& Steelmaking , 1997, Vol.24, No.4, pp. 300-305.

[6] M.M. Nzotta, Du Sichen and S. Seetharaman, Sulphide capacities in some multi component slag systems, ISIJ International, 1998, Vol.38, No.11, pp.1170-1179.

[7] J.A. Duffy and M.D. Ingram, "Establishment of an Optical Scale for Lewis Basicity in Inorganic Oxyacids, Molten Salts and Glasses", J. Am. Ceram. Soc., 1971, Vol.93, pp. 6448-6454.

[8] J.A. Duffy, M.D. Ingand I.D. Sommerville, "Acid/Basic Properties of Molten Oxides and Metallurgical Slags", J. Chem. Soc. Faraday Trans., 1978, Vol.74, No.6, pp. 1410-1419.

[9] I.D. Sommerville and Y.D.Yang, “Basicity of Metallurgical Slags”, AusIMM Proceedings, Vol.306, No.1, 2001, pp. 71-77.

[10] D.J. Sosinsky and I.D. Sommerville, "The Composition and Temperature Dependence of the Sulphide Capacity of Metallurgical Slags", Met. Trans. B, 1986, Vol.17B, pp.331-337.

[11] Y.D. Yang, I.D. Sommerville and A. McLean, "Some Fundamental Considerations Pertaining to Oxide Melt Interactions and Their Influence on Steel Quality", Trans. Indian Inst. Met., 2006, Vol.59, No.5, pp.655-669.

[12] G. Effenberg& S. Llyenko, "Ternary Alloy System", LANDOLT–BORNSTIEN Numerical Data and Functional Relationship in Science & Technology, Vol.11, Part II, Springer, p. 224.

[13] D.J. Min and N. Sano, Determination of Standard Free Energies of Formation ofCa3P2and Ca3Sn at High Temperatures, Metallurgical Transactions B, 1988, Vol.19B,pp. 433-439.

[14] D.J. Min and N. Sano, Determination of the Standard Gibbs Energies of Formationof Ca3As2, Ca3Sb2and Ca3Bi2, Metallurgical Transactions B, 1989, Vol.20B, pp. 863-869.

[15] Y.C. Dong, Z.P. Shi, L.M. Zhang, Y.Q. Peng and Y.R. Hong, Study on Dearsenization of Molten Iron, Iron & Steel, 1984, Vol.19, No.9, pp.1-6 (in Chinese).

[16] S.P. Liu and S.C. Sun, A Study on Dearsenization of Molten Iron and Liquid Steel with CaSi Alloy, Special Steel, 2001, Vol.22, No.5, pp.12-14 (in Chinese).